Low-energy phonon structure of ^{150}Sm

H. G. Börner,[1] P. Mutti,[1] M. Jentschel,[1] N. V. Zamfir,[2,3] R. F. Casten,[2] E. A. McCutchan,[2] and R. Krücken[2,4]
[1]*Institut Laue-Langevin, F-38042 Grenoble, France*
[2]*WNSL, Yale University, New Haven, Connecticut 06520, USA*
[3]*National Institute of Physics and Nuclear Engineering, Bucharest-Magurele, Romania*
[4]*Physik Department E12, Technische Universität München, D-85747 Garching, Germany*
(Received 12 January 2006; published 21 March 2006)

The low-lying decay scheme of ^{150}Sm is studied through the (n,γ) reaction. Precise energies as well as lifetimes measured with the gamma-ray-induced Doppler technique provide important structural information. A comparison with the predictions of interacting boson model calculations confirms that this nucleus is very close to the phase transition between spherical and quadrupole axial symmetric shapes, lying just prior to the critical point on the spherical side of the transition.

DOI: 10.1103/PhysRevC.73.034314 PACS number(s): 21.10.Re, 21.10.Tg, 21.60.Fw, 27.70.+q

I. INTRODUCTION

The nature and evolution of collectivity and coherence in atomic nuclei is one of the most fundamental issues in nuclear structure. One of the long-persisting issues that has been under intense study in recent years is whether finite nuclei can exhibit phase coexistence and phase-transitional behavior of the type observed in other physical systems. It has long been thought that true phase-transitional behavior was impossible, at least at low excitation energies where the level densities are low and states are discrete.

Recent evidence [1–3], however, in ^{152}Sm suggests that phase transitions and phase coexistence may indeed exist in atomic nuclei. Level sequences representing deformed (yrast levels) and spherical-type states (those built on the 0_2^+ level) have been identified. These coexisting deformed and spherical structures have been reproduced in both interacting boson approximation (IBA) model and geometric collective model (GCM) calculations [4,5] using a single Hamiltonian and a single set of basis states. These results prompted the development of the X(5) critical point model [6] to describe nuclei at the critical point of the phase transition from spherical to axially deformed shapes. The X(5) solution is obtained by solving the Bohr Hamiltonian with an infinite square well potential in the β deformation. The predictions involve a more deformed ground-state structure and a less deformed band built on the 0_2^+ level. ^{152}Sm was the first nucleus proposed [7] to exhibit a structure close to the X(5) predictions.

The observation of evidence for phase coexistence does not in itself define a phase transitional region. However, other approaches to nuclear systematics have been used [8–10] that circumvent the problem that nuclei are finite and change by discrete (integer) values of nucleon number. Nevertheless, a complete study of phase-transitional behavior requires an understanding of structure both before and after the phase-transitional point. With ^{152}Sm having been identified as a nucleus close to the phase-transitional point, a natural choice to study the evolution of structure surrounding the phase-transitional region is the nucleus ^{150}Sm. Despite the numerous studies devoted to the Sm isotopes, there still is the need for key empirical results on γ-ray branching ratios and absolute $E2$ matrix elements.

The purpose of this study is to provide a very precise decay scheme of ^{150}Sm populated in the (n, γ) reaction. Precise γ-ray energies are measured using the ultrahigh resolution GAMS4 flat crystal spectrometer [11] and level lifetimes are determined using the gamma-ray-induced Doppler (GRID) technique [12]. The resulting decay scheme is interpreted in terms of the IBA model and the location of ^{150}Sm relative to the phase-transitional point is discussed.

II. MEASUREMENTS AND RESULTS

States in ^{150}Sm were populated in the (n, γ) reaction at the high flux reactor of the Institut Laue-Langevin (ILL) in Grenoble. The target consisted of natural Samarium, for which about 98% of the thermal capture cross section (41000b)is on ^{149}Sm. It was placed 50 cm away from the reactor core, where the neutron flux was 5×10^{14} n cm^{-2} s^{-1}. γ rays were detected with the ultra-high-resolution GAMS4 flat crystal spectrometer [11,12]. The spectrometer provided the opportunity to obtain both highly precise transition energies as well as level lifetimes in ^{150}Sm.

A. High-precision energies

Transition energies were measured with the GAMS4 spectrometer by detection of the Bragg diffraction angle of the γ ray of interest from Si crystals. The energy resolution of this spectrometer is on the order of 10^{-6} (a few electron volts for 1-MeV transitions). The technique and the spectrometer have been described elsewhere [11,12]. The energies of many transitions were measured with high precision and enabled: (i) the determination if a γ-ray transition is correctly placed and (ii) the measurement of level energies, sometimes using different γ-decay paths, with very high accuracy

Table I lists the energies of all of the γ-ray transitions measured in the present work. Additional previously observed transitions are included from Ref. [13]. The energies of the

 ©2006 The American Physical Society

TABLE I. Levels in ^{150}Sm studied in this work and their γ decay.

J_i^π	E_i (keV)	J_f^π	E_γ [a] (keV)	I_γ [b]
2_1^+	333.9514(8)	0_1^+	333.9514(8)	100
0_2^+	740.4652(11)	2_1^+	406.5156(8)	100
4_1^+	773.3726(9)	2_1^+	439.4227(9)	100
2_2^+	1046.1464(8)	0_1^+	1046.1459(21)	8(1)
		2_1^+	712.1918(14)	100(6)
		0_2^+	305.6813(6)	2.5(5)
3_1^-	1071.3957(9)	2_1^+	737.4420(15)	100(2)
		4_1^+	298.061(14)[b,c]	6.71(9)
1_1^-	1165.7770(10)	0_1^+	1165.739(27)	100(4)
		2_1^+	831.8235(17)	75(3)
2_3^+	1193.8405(10)	0_1^+	1193.8412(24)	100(10)
		2_1^+	859.8846(17)	85(8)
		0_2^+	453.3772(9)	4.1(8)
		4_1^+	420.48(9)[b]	1.3(4)
		2_2^+	147.73(4)[b]	0.15(8)
0_3^+	1255.4985(19)	2_1^+	921.5471(18)	100(20)
		2_2^+	209.36(2)[b]	10(3)
6_1^+	1278.8995(13)	4_1^+	505.5269(10)	100
5_1^-	1357.6615(9)	4_1^+	584.2902(11)	100(3)
		3_1^-	286.293(15)[b,d]	0.19(3)
		6_1^+	78.76(1)[b]	0.16(2)
2_4^+	1417.3404(8)	0_1^+	1417[b]	0.06(4)
		2_1^+	1083.4152(200)[e,f]	70(8)
		3_1^-	345.9434(7)	100(10)
		1_1^-	251.5632(5)	46(4)
		2_3^+	223.5012(4)	1.7(3)[g]
		0_3^+	161.84(3)[b,h]	3(1)
4_2^+	1449.1778(8)	4_1^+	675.8057(14)	100(2)
		2_2^+	403.0316(8)	45(5)
		3_1^-	377.73(3)[b,c]	3.0(3)
		2_3^+	255.3362(5)	1.06(15)
		6_1^+	170.23(2)[b,c,h]	0.26(4)
		5_1^-	91.8(4)[b,h]	0.19
3_1^+	1504.5635(9)	2_1^+	1170.6108(23)	100(1)
		4_1^+	731.1909(15)	25.2(7)
		2_2^+	458.4167(9)	3.3(4)
		2_3^+	310.7233(6)	2.2(4)
4_3^+	1642.6457(9)	2_1^+	1308.6921(26)	38(4)
		4_1^+	869.2747(17)[d]	100(1)
		2_2^+	596.53(4)[b]	2.2(4)
		3_1^-	571.2512(10)	21(2)
		2_3^+	448.8037(9)	11(2)
		5_1^-	284.9843(6)	9(1)
		2_4^+	225.34(2)[b,c]	0.32(6)
		4_2^+	193.46(2)[b]	0.6(1)
		3_1^+	138.05(4)[b,h]	0.08(4)
(4_4^+)	1673.1775(20)[i]	4_1^+	899.8049(18)[f]	100(80)
		2_2^+	626.67(22)[b,c]	80(60)
4_5^+	1819.4375(12)	2_1^+	1485.4919(30)	37(2)
		2_2^+	773.2921(15)[d]	11.7(2)
		3_1^-	748.0430(15)	100(2)
		2_3^+	625.568(20)[b]	5.98(13)
		6_1^+	540.55(6)[b]	1.67(13)
		5_1^-	461.7766(9)	15.9(4)
		2_4^+	402.0986(8)	15.1(2)
		4_2^+	370.2575(7)	2.07(17)
		3_1^+	315.0(2)[b]	0.33(11)
4_6^+	1821.9253(10)	6_1^+	542.972(25)[b]	40(7)
		5_1^-	464.2638(9)	100(17)
		4_2^+	372.7475(8)	62(7)
		4_3^+	179.26(5)[b]	0.40(21)
8_1^+	1837.0126(17)[i]	6_1^+	558.1131(10)[f]	100

[a]The energies are relative to the 333.9-keV $2_1^+ \rightarrow 0_1^+$ transition, fixed as 333.9514 keV. Only the systematic uncertainties are given.
[b]From NDS.
[c]Within 2σ of the energy difference.
[d]Multiply placed in NDS.
[e]The statistical uncertainty is included.
[f]Placement uncertain.
[g]Multiply placed in NDS, undivided intensity given.
[h]Placement uncertain in NDS.
[i]The existence of the level is based only on one transition.

majority of the newly measured γ-ray transitions confirm their previous placement (see Table I). There are, however, several transitions for which the present work finds no evidence for their placement. Table II lists the expected energies for these transitions (as the difference between the energies of the levels between which they were previously placed) and the present, precise γ-ray energy. As evident from Table II, with the new very precise energies, the previous placements are no longer valid. We discuss later the consequences for nuclear structure.

B. The GRID technique

A nucleus formed in thermal neutron capture is in a highly excited state close to the neutron separation energy. Such a nucleus will deexcite mostly by a cascade of γ rays. The emission of each γ ray induces a small but detectable recoil to the nucleus. The measured γ rays will be Doppler broadened rather than shifted as the directions of the initial recoils are uniformly distributed. Because the recoil energies are very small, $v/c < 10^{-4}$, the observation of Doppler broadening demands extraordinarily high resolution that can be achieved by using the ultra-high-resolution GAMS4 flat crystal spectrometer.

The experimental data measured by the instrument is the line-shape profile of a γ ray that depends on the instrument response and the Doppler broadening. The latter depends on the decay pattern of the nucleus, the lifetimes of nuclear states involved in the decay, and the slowing-down process of the recoiling nucleus. If all these effects are properly considered [12], it is possible to extract the lifetime τ for the level of interest. This method is known as the GRID method [12].

The major uncertainty in extracting a level lifetime with the GRID technique is actually not directly the result of the measured linewidth itself but rather because of estimating the initial recoil velocity distribution at the time of population of the level of interest. This velocity distribution depends on the energy distribution of the γ-ray feeding levels from the capture state and the lifetimes of the intermediate levels.

By inspecting the population-depopulation balance for the level of interest, the missing populating intensity can be

TABLE II. γ transitions that had previously been placed but the present study finds no evidence for that placement.

E_γ (keV)		E_i[a] (keV)	E_f[a] (keV)	$E_i - E_f$ (keV)
Ref. NDS	Present			
272.82(3)[b]	272.8236(6)	1046.1464(8)	773.3726(9)	272.7738(12)
425.10(7)		1165.7770(10)	740.4652(11)	425.312(2)
370.721(25)	370.7285(7)	1417.3404(8)	1046.1464(8)	371.1940(11)
393.92(5)[c]		1673.1775(20)	1278.8995(13)	394.278(2)
223.51(2)[b,c]			1449.1778(8)	223.9997(2)
168.24(4)[c]			1504.5635(9)	168.614(2)
1045.873(12)[b,c]	1045.714(2)	1819.4375(12)	773.3726(9)	1046.0649(13)
135.05(17)			1684.000(17)[d]	135.437(2)

[a]From present work.
[b]Multiply placed.
[c]Placement uncertain.
[d]From Ref. NDS.

estimated. The upper limit of τ corresponds to the highest recoil velocities and is obtained by assuming that all unobserved feeding is via a two-step cascade from the neutron capture state with intermediate level lifetime $\tau = 0$. (It is known that single step population by primary transitions is very weak.) Then, a given Doppler broadening for a depopulating γ-ray will correspond to the longest slowing down time before γ-ray emission and therefore to the longest lifetime. The lower limit on the lifetime comes from assuming that all the feeding of each level comes from a state of effectively infinite lifetime (hence the nucleus emitting the feeding γ-ray has no initial recoil velocity) at the lowest possible energy consistent with the level scheme.

An example of a Doppler broadened line shape is given in Fig. 1 for the 712-keV transition depopulating the 2_2^+ state in ^{150}Sm. From an analysis of the instrumental and observed line shapes, the extreme feeding assumptions give a lifetime for the 2_2^+ state of 1.220 ps $< \tau <$ 2.754 ps.

The lifetimes measured in the present work are given in Table III. The lifetime of two levels were measured before in a Coulomb excitation experiment [13,14]: $1.24^{+0.45}_{-0.30}$ ps for the 2_2^+ state and 1.88(43) ps for the 2_3^+ state. The new range of values for the 2_2^+ state is in agreement with the previous measurement, whereas the measured lifetime for the 2_3^+ state (0.625–1.156 ps) is a factor of 2–3 smaller than the literature value.

III. IBA

The transitional region of Sm ($N > 82$) has been successfully studied in the framework of the IBA as a transition from U(5) to SU(3) [15,16]. The structural signature $R_{4/2} \equiv E(4_1^+)/E(2_1^+)$ for ^{150}Sm is 2.32, between 2.00, the spherical vibrator limit and 3.0 the shape/phase transition point to quadrupole deformed nuclei [4,10]. The IBA Hamiltonians used in fitting the Sm isotopic chain range from the most

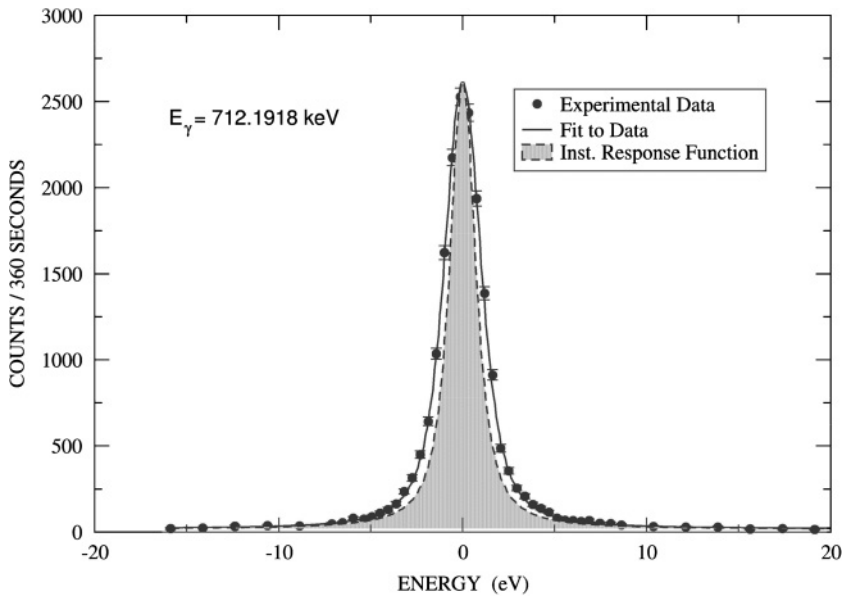

FIG. 1. The Doppler broadened line shape for the 712-keV transition. The dotted line shows the instrumental linewidth. The solid line is a fit to the data that incorporates Doppler broadening because of the finite lifetime.

TABLE III. Mean lifetimes measured in this work deduced from extreme feeding assumptions.

J^π	E_x (keV)	E_γ (keV)	$\tau_{\min}-\tau_{\max}$ (ps)
2_2^+	1046	712	1.220–2.754
3_1^-	1071	737	0.298–0.502
1_1^-	1166	1166	0.057–0.289
		832	0.072–0.244
2_3^+	1194	1194	0.625–1.156
6_1^+	1279	506	2.414–4.426
4_2^+	1449	676	1.494–3.626
4_3^+	1643	869	0.428–1.137
8_1^+	1837	558[a]	0.779–2.882[b]

[a]Placement uncertain.
[b]The lifetime deduced for this level is meaningful only if the measured 558-keV transition is correctly placed.

simple one [15], along the U(5)-SU(3) leg of the symmetry triangle, to the most general up to two-body terms [16]. Here, we compare the experimental results with the predictions of the detailed calculations of Ref. [15] where small adjustments to the simplest Hamiltonian are introduced:

$$H = \epsilon n_d - \kappa Q \times Q + \kappa' L \times L - \kappa'' P^\dagger P, \qquad (1)$$

where $n_d = (d^\dagger \times \tilde{d})$ and $Q = [d^\dagger \tilde{s} + s^\dagger \tilde{d}]^{(2)} - \frac{\sqrt{7}}{2}[d^\dagger \tilde{d}]^{(2)}$, $L = \sqrt{10}[d^\dagger \tilde{d}]^{(1)}$, and $P^\dagger = (^1/_2)(s^\dagger s^\dagger + d^\dagger \times d^\dagger)$.

The parameters for ^{150}Sm are $\epsilon = 0.384$ keV, $\kappa = 0.01$ keV, $\kappa' = 0.0005$ keV, and $\kappa'' = 0.0526$ keV [15]. Figure 2 presents the comparison of the empirical low-lying spectrum of ^{150}Sm with the IBA calculations. A phononlike structure is evident in both the experimental spectrum and the IBA calculations. The anharmonicities observed in both the two-phonon and three-phonon multiplet are well reproduced by the IBA calculations. Experimentally, a single excited 0^+ state is observed around the three-phonon multiplet energy, whereas the IBA predicts two closely spaced 0^+ states at a similar energy. The phonon nature of these states and the structure of the excited 0^+ states are discussed in the next section. Figure 3 shows the corresponding total energy of the system obtained with these IBA parameters using the intrinsic state formalism [17], as a function of the quadrupole deformation, $\beta_{\rm IBA}$. The energy presents a shallow minimum at zero quadrupole deformation showing that the system behaves, indeed, as an anharmonic spherical vibrator.

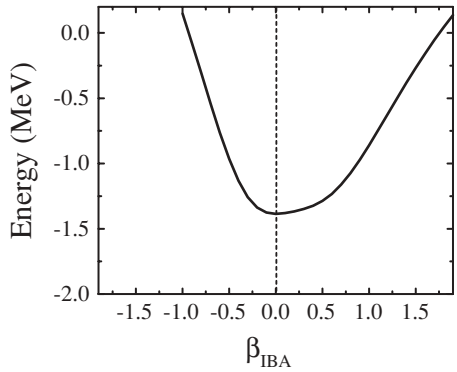

FIG. 3. Total energy of the system corresponding to the IBA Hamiltonian in Eq. (1) with $\epsilon = 0.384$ keV, $\kappa = 0.01$ keV, $\kappa' = 0.0005$ keV, and $\kappa'' = 0.0526$ keV.

IV. DISCUSSION

A more complete interpretation of the phonon structure of a level can be obtained by considering electromagnetic transition probabilities. For the $B(E2)$ values determined in the present work, in order to simplify the discussion, we will use an experimental mean $B(E2)$ value calculated as the average of the $B(E2)$ values determined using the extreme lifetimes in Table III. The uncertainties are given by the deviations between the mean value and the value calculated using the extreme lifetimes. The uncertainty in the experimental value of the relative intensity is also included. For the spin unchanging transitions where the multipole mixing ratio is not measured,

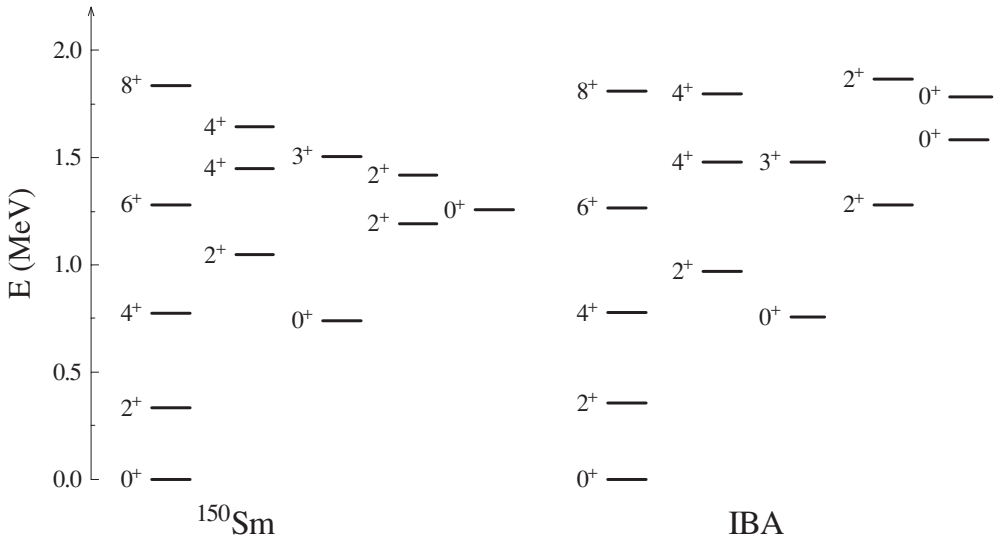

FIG. 2. Comparison of experimental low-lying energy levels in ^{150}Sm with the IBA calculations.

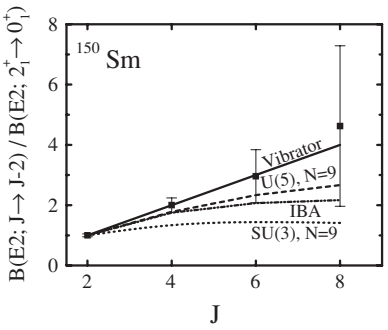

FIG. 4. $B(E2; J \rightarrow J-2)$ values for yrast states normalized to $B(E2; 2_1^+ \rightarrow 0_1^+)$ compared with harmonic vibrator, U(5), SU(3), and the IBA predictions of Ref. [15].

pure $E2$ character is taken in the calculation of the $B(E2)$ value and indicated by an upper limit. The $B(E2)$ values for the $2_1^+ \rightarrow 0_1^+$, $4_1^+ \rightarrow 2_1^+$, and $0_2^+ \rightarrow 2_1^+$ transitions are from a previous Coulomb excitation measurement [13,14].

The $B(E2)$ values in the yrast sequence, shown in Fig. 4, present a trend characteristic of a spherical harmonic vibrator, although, considering the large experimental uncertainties, an anharmonic vibrator behavior such as in the IBA description is not excluded.

A comparison of the decay scheme of the two-quasiphonon triplet 4_1^+, 2_2^+, and 0_2^+ with the IBA results is shown in Fig. 5. The strong decays from the members of the two-quasiphonon triplet to the one-quasiphonon 2_1^+ level as well as the weak $2_2^+ \rightarrow 0_1^+$ transition (forbidden in a phonon scheme) are well reproduced by the calculations. A strong decay of the 2_2^+ state to the 0_2^+ state is found in the data, although with significant uncertainty. The IBA calculations reproduce the

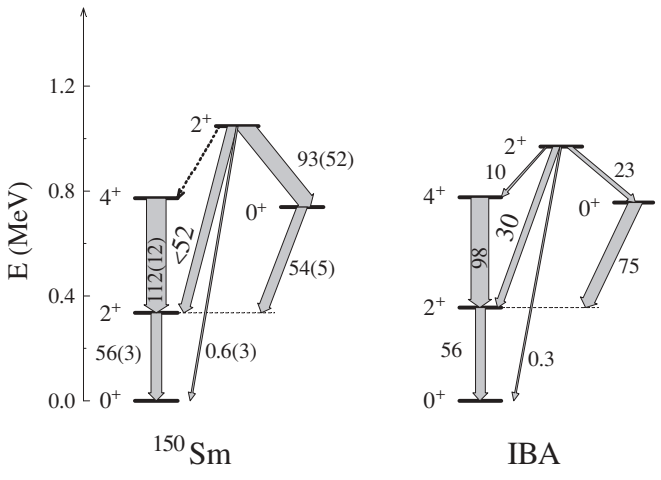

FIG. 5. Experimental absolute $B(E2)$ values (in W.u.) compared with the IBA predictions for transitions from the 4_1^+, 2_2^+, and 0_2^+ levels belonging to the two-quasiphonon multiplet. The experimental values are calculated using the mean value of the lifetimes deduced from extreme feeding assumption from Table III (see text). The uncertainties are in fact deviations of these values to the value calculated with the extreme lifetimes. The thicknesses of the transition arrows are proportional to the $B(E2)$ value.

relative magnitude of this transition yet the absolute strength is somewhat underestimated. The transition from 2_2^+ to 4_1^+, according to the present precise energy measurements, should have an energy of 272.7738(12) keV. In the present work, a γ ray with energy 272.8236(6) keV was observed (see Table I) and, consequently, there is no evidence for a transition between these two levels. In fact, the previous transition assigned between these two levels [13] had an energy of 272.82(3) keV and was doubly placed. The IBA predicts $B(E2; 2_2^+ \rightarrow 4_1^+) = 10$ W.u., which would correspond to a relative intensity $I(2_2^+ \rightarrow 4_1^+)/I(2_2^+ \rightarrow 0_1^+) = 0.04$, which is significantly smaller than the intensity of 0.17 reported in Ref. [13].

A comparison of the decay properties of the three-quasiphonon multiplet members measured in the present work (6_1^+, 4_2^+, and 2_3^+) with the IBA predictions is shown in Fig. 6. The branching properties of the 2_3^+ state are reasonably described by the IBA calculations. Good agreement is obtained in the strength of the decay of the 2_3^+ state to the 4^+ and 0^+ members of the two-quasiphonon multiplet. The IBA predicts a transition of similar strength in the decay to the 2_2^+ state. This transition is tentatively assigned to have $M1$ multipolarity in Ref. [13]. If this is indeed a pure $M1$ transition, then the IBA significantly overpredicts the strength. The decays to the 2_1^+ and 0_1^+ states that would be forbidden transitions in a phononlike scheme are more suppressed in the IBA calculations than is seen in the experimental data. The IBA predictions for the decay of the 4_2^+ state show less agreement with the experimental data compared with the 2_3^+ decay. Overall, the strong experimental transitions are significantly underpredicted by the IBA calculations. However, although the overall scale is underpredicted, the relative branchings from the 4_2^+ state are reproduced by the calculations.

As seen in Fig. 2, the calculations predict two closely spaced 0^+ states above the two-phonon triplet. These states exhibit different structures. Figure 7 (top) gives the calculated wave functions of the 0^+ states as a distribution of squared amplitudes in terms of n_d. Their structure is not very simple in terms of a phononlike structure but a few characteristics can be extracted. The first 0^+ state has the main component with $n_d = 0$ that is expected for a quasispherical nucleus. The most likely member of the two-phonon triplet, considering the excitation energy, is the 0_2^+ state (see Fig. 2). The 0_4^+ state has the main component $n_d = 3$, which corresponds to the three-phonon multiplet. The 0_3^+ state has no correspondence in the phononlike picture and could correspond to a deformed shape coexisting with the spherical ground-state structure [4]. This is supported by the expectation value of n_d in the 0_3^+ state, which is 4.5, compared with a value of 4.9 for the expectation value of n_d in the ground state 0^+ in the SU(3) limit. To establish the empirical 0^+ state corresponding to this "deformed" structure, we compare in Fig. 8 the known empirical information on the third 0^+ state, namely the decay branching ratio to 2_1^+ and 2_2^+ states, with the IBA predictions for the 0_3^+ and 0_4^+ states. It is evident that the empirical 0_3^+ state resembles the calculated 0_3^+ state that, as shown above, corresponds to a "deformed" structure. A possible candidate for the 2^+ state corresponding to the 0_3^+ state is a 2_4^+ state that decays to the 0_3^+ state. However,

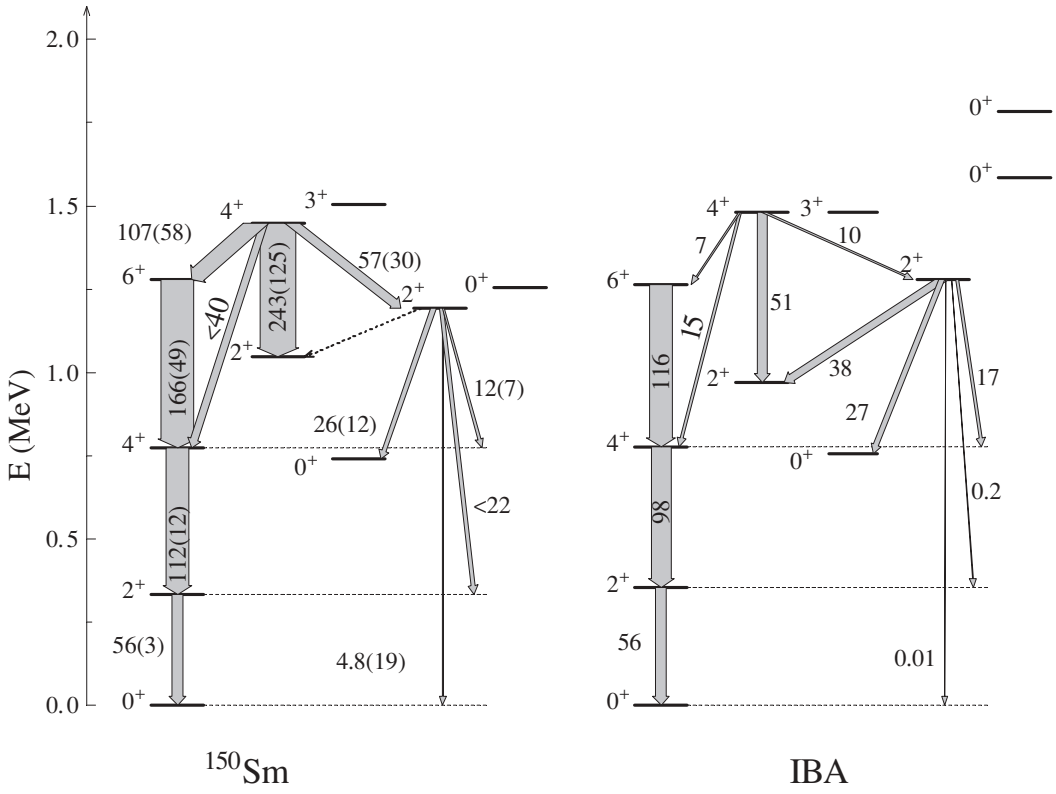

FIG. 6. Same as Fig. 5 but for the transitions from the 6_1^+, 4_2^+, and 2_3^+ levels belonging to the three-quasiphonon multiplet.

the IBA calculation predicts only a small transition strength: $B(E2; 2_4^+ \rightarrow 0_3^+) = 12$ W.u. This is somehow understandable because of the composition of wave functions of the 2^+ states as seen in Fig. 7 (bottom). Unfortunately, this transition probability is not known experimentally, which makes the conclusion difficult.

From the above analysis, the energies and decay strengths suggest that the 4_1^+, 2_2^+, and 0_2^+ states are members of the two-quasiphonon multiplet, whereas the 6_1^+, 4_2^+, and 2_3^+ states are members of the three-quasiphonon multiplet. This establishes the ground state of ^{150}Sm as close to a spherical vibrator. The identification of the 0_3^+ state as possibly corresponding to a

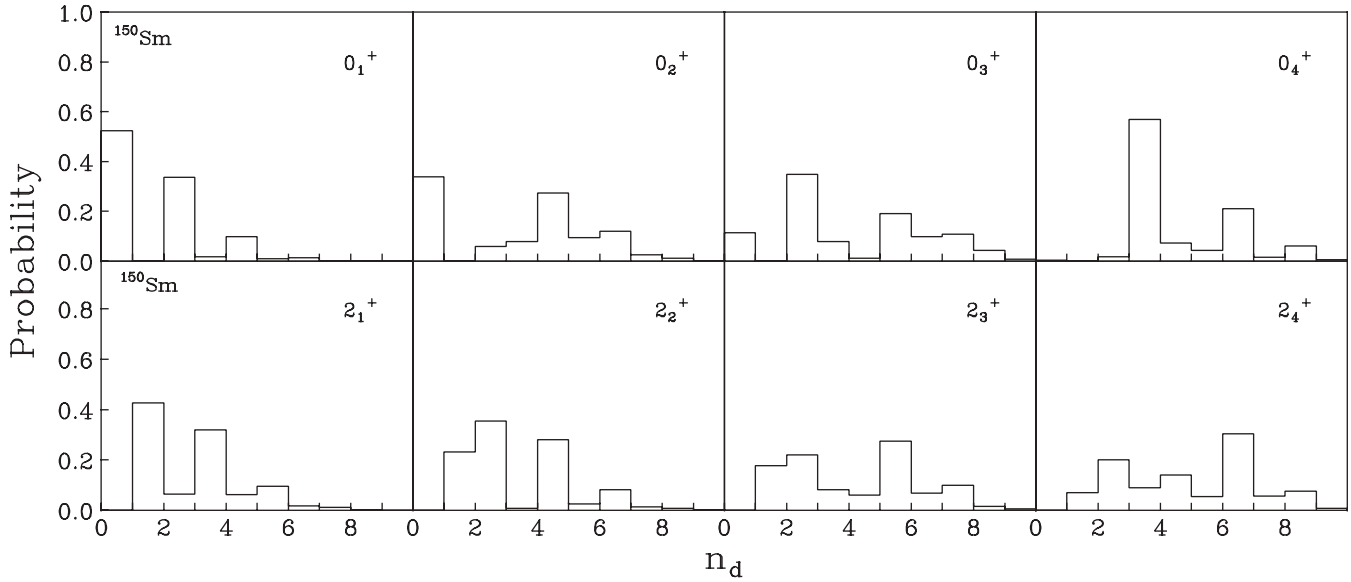

FIG. 7. Distribution of squared wave-function amplitudes for the first four 0^+ and 2^+ states as a function of n_d from the IBA calculations of Ref. [15].

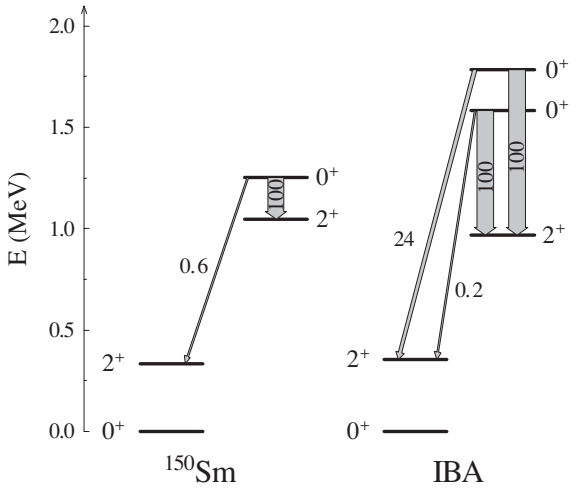

FIG. 8. Comparison of the known relative $B(E2)$ values for the decay of the 0_3^+ state in ^{150}Sm with the IBA calculations for the 0_3^+ and 0_4^+ states.

deformed structure would indicate that the character of the level sequences in ^{150}Sm is opposite to that of ^{152}Sm, with a spherical ground state and a deformed excited state structure. This suggests that ^{150}Sm is located before the phase-transitional point in the evolution from spherical to deformed structures.

V. CONCLUSION

Spectroscopic information, energies, and lifetimes on low-lying states in ^{150}Sm were obtained using the (n, γ) reaction. By comparing the existing data with detailed IBA calculations, we identified the quasispherical phonon structure of this nucleus and a possible coexisting deformed 0^+ state.

ACKNOWLEDGMENT

Work supported by the U.S. DOE by grant DE-FG02-91ER-40609.

[1] R. F. Casten, M. Wilhelm, E. Radermacher, N. V. Zamfir, and P. von Brentano, Phys. Rev. C **57**, R1553 (1998).
[2] N. V. Zamfir, R. F. Casten, M. A. Caprio, C. W. Beausang, R. Krucken, J. R. Novak, J. R. Cooper, G. Cata-Danil, and C. J. Barton, Phys. Rev. C **60**, 054312 (1999).
[3] T. Klug, A. Dewald, V. Werner, P. von Brentano, and R. F. Casten, Phys. Lett. **B495**, 55 (2000).
[4] F. Iachello, N. V. Zamfir, and R. F. Casten, Phys. Rev. Lett. **81**, 1191 (1998).
[5] J. Y. Zhang, M. A. Caprio, N. V. Zamfir, and R. F. Casten, Phys. Rev. C **60**, 061304(R) (1999).
[6] F. Iachello, Phys. Rev. Lett. **87**, 052502 (2001).
[7] R. F. Casten and N. V. Zamfir, Phys. Rev. Lett. **87**, 052503 (2001).
[8] R. F. Casten, N. V. Zamfir, and D. S. Brenner, Phys. Rev. Lett. **71**, 227 (1993).
[9] A. Wolf, R. F. Casten, N. V. Zamfir, and D. S. Brenner, Phys. Rev. C **49**, 802 (1994).
[10] R. F. Casten, D. Kusnezov, and N. V. Zamfir, Phys. Rev. Lett. **82**, 5000 (1999).
[11] E. G. Kessler *et al.*, J. Phys. G **14**, S167 (1988).
[12] H. G. Börner and J. Jolie, J. Phys. G **19**, 217 (1993).
[13] E. der Mateosian and J. K. Tuli, Nucl. Data Sheets **75**, 827 (1995).
[14] R. J. Keddy, Y. Yoshizawa, B. Elbek, B. Herskind, and M. C. Olesen, Nucl. Phys. **A113**, 676 (1968).
[15] O. Scholten, F. Iachello, and A. Arima, Ann. Phys. (N.Y.) **115**, 325 (1978).
[16] J. E. Garcia-Ramos, J. M. Arias, J. Barea, and A. Frank, Phys. Rev. C **68**, 024307 (2003).
[17] J. N. Ginocchio and M. W. Kirson, Nucl. Phys. **A350**, 31 (1980).